

Original paper

Szilagyiite, a new uranyl carbonate-selenite mineral related to schröckingerite from the Pickett Corral mine, Montrose County, Colorado, USA

Travis A. OLDS^{1*}, Christopher EMPROTO¹, Anthony R. KAMPF², Chi MA³, and Joe MARTY²

¹ Section of Minerals and Earth Sciences, Carnegie Museum of Natural History, 4400 Forbes Avenue, Pittsburgh, Pennsylvania 15213, USA, oldst@carnegiemnh.org

² Mineral Sciences Department, Natural History Museum of Los Angeles County, 900 Exposition Boulevard, Los Angeles, CA 90007, USA, akampf@nhm.org

³ Division of Geological and Planetary Sciences, California Institute of Technology, 1200 East California Boulevard, Pasadena, California 91125, USA

* Corresponding author



Szilagyiite (IMA 2024-063), $\text{NaCa}_3(\text{UO}_2)(\text{CO}_3)_3(\text{SeO}_3)\text{F}(\text{H}_2\text{O})_6$, is a new uranyl-carbonate-selenite mineral from the Pickett Corral mine, Montrose County, Colorado, USA. The new mineral occurs on sandstone and asphaltite matrix in close association with ferroselite, andersonite, schröckingerite, magselite, and an unidentified Na-Ca-uranyl carbonate-selenite-sulfate. Szilagyiite is trigonal, space group $R3c$ (#161), with unit cell parameters $a = 9.6542(9)$, $c = 33.465(5)$ Å, $V = 2701.2(6)$ Å³ and $Z = 6$. Crystals occur as dense yellow-green rosettes up to 1 mm wide and individual tablets up to ~200 µm. Szilagyiite crystals are predominantly tabular on {001} and exhibit {001}, {00-1}, {102}, and {0-1-2} forms, with frequent twinning by inversion and perfect {001} cleavage. It has a pale yellow-green streak and fluoresces dimly green under longwave UV and 405 nm illumination, but has no apparent fluorescence under SWUV. Crystals are transparent with vitreous luster and exhibit a brittle, uneven fracture, with a Mohs hardness between 2–3. The calculated density based on the empirical formula is 3.17 g/cm³, and 3.16(2) g/cm³ as measured by flotation in a mixture of diiodomethane and toluene. The mineral is optically uniaxial (–), with $\omega = 1.628(2)$, $\epsilon = 1.538(2)$ measured in white light. It is pleochroic: O yellow, E colorless; $O > E$. The empirical formula is $\text{Na}_{0.76}\text{Ca}_{3.11}(\text{UO}_2)(\text{CO}_3)_3(\text{Se}_{1.16}\text{O}_3)\text{F}_{0.82}\text{O}_{20.18}\text{H}_{13.19}$ based on 21 O + F, $U = 1$, with $C = 3$ apfu based on the structure and H set to achieve charge balance. The eight strongest powder X-ray diffraction lines are [d_{obs} Å(1)(hkl)]: 5.916(100)(104), 4.836(58)(110), 3.744(77)(018), 3.125(33)(211,122), 2.960(60)(214), 2.795(62)(300), 1.828(40)(410) and 1.744(35)(238,146). The structure of szilagyiite ($R_1 = 0.0314$ for 2335 reflections with $I > 2\sigma I$) is based on infinite sheets built from 3 major components: distorted cubane-like $[(\text{SeO}_3)\text{Ca}_3(\text{F},\text{OH})(\text{H}_2\text{O})_3]$ units, $\text{NaO}_4(\text{H}_2\text{O})_3$ monocapped trigonal antiprisms, and hexagonal bipyramidal uranyl tricarbonate cluster units, $[\text{UO}_2(\text{CO}_3)_3]$. The sheets are cross-linked by a thin layer of hydrogen bonds formed between interlayer H_2O bound to Na, with F/OH, and O in the sheets.

Keywords: Szilagyiite, uranyl carbonate-selenite, uranium, crystal structure, schröckingerite, Raman

Received: 5 December 2025; **accepted:** 6 January 2026; **handling editor:** J. Plášil

The online version of this article (doi: 10.3190/jgeosci.0049.25) contains supplementary electronic material.

We dedicate this paper to the memory of Ing. Jiří Čejka, DrSc. (1929–2025) who co-authored many of the new uranyl minerals from Utah and Colorado.

1. Introduction

The primary mobilizer of the uranyl ion in groundwater is the carbonate anion, forming some of the most stable aqueous U^{6+} species known (Gorman-Lewis et al. 2008). Though highly soluble, uranyl carbonate species rank midway in number (~43) among known uranium minerals containing common oxyanions; there are marginally more sulfates (~53) and phosphates (~50), and slightly fewer arsenates (~37), but about half as many silicates (~24), and vanadates (~17). Poly-anionic carbonates are even rarer and include the two

ultra-rare carbonate-silicates lepersonnite-(Gd), -(Nd) and the carbonate-sulfate ježekite, so far known as a single-locality species. A fourth, the carbonate-sulfate schröckingerite, is a very commonly encountered post-mining mineral in uranium mines worldwide. Generally, this is because the ~circumneutral to mildly basic conditions required for the formation of uranyl carbonates lies outside the solubility and redox fields of most other oxyanions in the presence of U. For example, uranyl vanadates are the solubility limiting species from pH ~6–8, where uranyl carbonates are often formed. Here we present szilagyiite, which is

closely related to schröckingerite and is the first uranyl carbonate-selenite fluoride.

Szilagyite (“zi-la-gee-ite”; /ˈzi:lɑːɡiːɑrt/) is named for Paul Szilagy (b. 1956), who helped collect the type material used in this study and provided access to the Blue Streak mining complex. Paul is CEO and Manager of Nuvemco, LLC, a Boulder, Colorado based company which he helped found in 2007, that is involved in development of the critical and strategic energy minerals uranium and vanadium. Nuvemco’s focus is the Uravan mineral belt and the company has acquired mineral rights on over 6,000 acres in Montrose County, Colorado and has obtained multiple state and federal mining permits. Paul also serves as a board member of the Western Small Miners Association. Paul has become an important advocate for mineralogical discovery, and actively supports the research and discovery of new minerals found on Nuvemco’s properties. Paul has given his permission for this namesake.

The mineral and its name have been approved by the Commission on New Minerals, Nomenclature and Classification of the International Mineralogical Association (IMA2024-063). The description is based on one holotype specimen deposited in the collections of the Carnegie Museum of Natural History, catalog number CM34760. The IMA-CNMNC approved mineral abbreviation for szilagyite is Szg (Warr 2021).

2. Occurrence

Szilagyite was collected underground from the Pickett Corral mine, Montrose County, Colorado, USA (38° 23' 02.4" N 112° 16' 27.2" W). The Pickett Corral is an inactive uranium and vanadium mine in the Uravan mineral belt of the Colorado Plateau. Its workings connect with the neighboring Blue Streak mine and each exhibit distinct secondary mineralogy. The Pickett Corral mine is notable as the type locality for several rare vanadate minerals including pseudodickthomssenite, $\text{Mg}(\text{VO}_3)_2 \cdot 8\text{H}_2\text{O}$, bicapite, $[\text{KNa}_2\text{Mg}_2(\text{H}_2\text{O})_{25}][\text{H}_2\text{PV}^{5+}_{12}\text{O}_{40}(\text{V}^{5+}\text{O})_2]$, and trebiskyite, $\text{Na}_3\text{Mg}_2[\text{TiV}_9\text{O}_{28}] \cdot 22\text{H}_2\text{O}$. (Kampf et al. 2019 and 2022a; Olds et al. 2024). These vanadates each occurred in distinct assemblages from that bearing szilagyite, which is the first uranium-bearing type species for the locality.

Sandstone-hosted uranium and vanadium mines are widespread in the Uravan mineral belt and contain differing concentrations of U–V ores with U primarily present as uraninite, UO_{2+x} , or coffinite, $\text{U}(\text{SiO}_4) \cdot n\text{H}_2\text{O}$, while V occurs predominantly as monroseite, $(\text{V}^{3+}, \text{Fe}^{2+}, \text{V}^{4+})\text{O}(\text{OH})$, and corvusite, $(\text{Na}, \text{Ca}, \text{K})_x(\text{V}^{5+}, \text{V}^{4+}, \text{Fe}^{2+})_8\text{O}_{20} \cdot 4\text{H}_2\text{O}$, or in sheet silicates such as vanadian clays or roscoelite, $\text{KV}^{3+}_2(\text{Si}_3\text{Al})\text{O}_{10}(\text{OH})_2$. Other

metals that may be enriched in these systems include Mo and Se, the latter typically occurs as an impurity in associated pyrite, and in some mines the element is known to occur relatively commonly as native Se, clausthalite (PbSe), and ferroselite (FeSe_2), among others.

The Uravan mineral belt encompasses sandstones of the Salt Wash member of the Triassic Morrison Formation within the Paradox Basin (Simandl and Paradis 2022). The original U and V ores, including abundant Fe and Cu as sulfides, were deposited when metal-laden groundwater encountered reducing conditions in the presence of abundant organic matter (asphaltite). These elements are leached from unmined ores and migrate through the porous siliciclastic units bearing a wide range of particle sizes from silt- and mudstones, to sandstones and conglomerates. In most cases, the strongest secondary mineralization occurs intimately within asphaltite layers and “pods.” In their oxidized forms, uranium and vanadium are highly soluble, redox-sensitive, and post-mining oxidation has produced highly diverse secondary mineralization throughout the Pickett Corral mine due to ongoing dissolution and recrystallization. Interestingly, through this process, some areas of the Pickett Corral mine walls and ceilings are coated nearly completely and homogeneously with 1–2 mm thick coatings of andersonite for tens of meters, indicating a strong dependence of the mineralogy on the air composition and flow rates. High CO_2 content, resulting from decomposition of calcite by acidic waters derived from decaying sulfides, coupled with periods of high humidity were likely necessary for the formation of szilagyite.

Szilagyite occurs in association with andersonite, $\text{Na}_2\text{Ca}(\text{UO}_2)(\text{CO}_3)_3 \cdot (5.333)\text{H}_2\text{O}$ (K. Mereiter pers. comm), schröckingerite, $\text{NaCa}_3(\text{UO}_2)(\text{CO}_3)_3(\text{SO}_4)\text{F} \cdot 10\text{H}_2\text{O}$, crusts of magselite, $[\text{Mg}(\text{H}_2\text{O})_6](\text{Se}^{4+}\text{O}_3)$, and a potentially new Na–Ca-uranyl carbonate-selenite-sulfate with a complex structure related to szilagyite and schröckingerite. Material containing szilagyite was extracted from a small

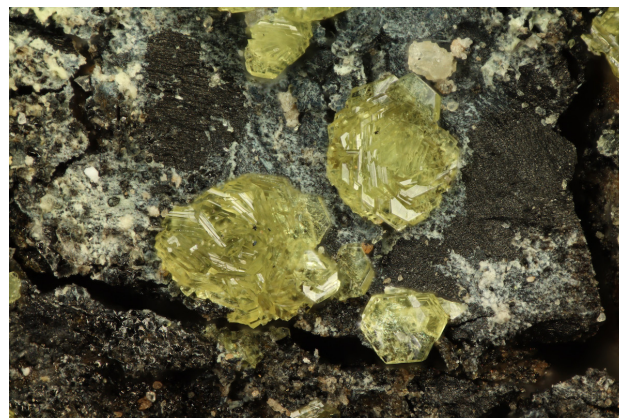


Fig. 1 Yellow green tablets and rosettes of szilagyite on asphaltite. Horizontal field of view is 2.25 mm.

(~0.25 m) asphaltite-laden sandstone lens richly coated by andersonite with sparse but dense patches of fine-grained ferroselite. The source of Se in szilagyiiite is clearly oxidized ferroselite, given its close association within several centimeters.

3. Physical and optical properties

Szilagyiiite occur as dense yellow-green rosettes up to 1 mm wide and subparallel tablets up to ~200 μm (Figs 1, 2). Szilagyiiite crystals are predominantly tabular on {001} and exhibit {001}, {00 $\bar{1}$ }, {102}, and {01 $\bar{2}$ } forms (Fig. 3), with frequent twinning by inversion and perfect {001} cleavage. It has a pale yellow-green streak and fluoresces dimly green under longwave UV and 405 nm illumination but does not fluoresce under SWUV. The low intensity of its fluorescence is a useful method to distinguish szilagyiiite from schröckingerite, which occurs as strongly fluorescent pseudo-hexagonal tabular crystals. Crystals are transparent with vitreous luster and exhibit a brittle, uneven fracture, with a Mohs hardness between 2 and 3. The calculated density based on the empirical formula is 3.17 g/cm^3 , and 3.16(2) g/cm^3 as measured by flotation in a mixture of diiodomethane and toluene.

The mineral is optically uniaxial (–), with $\omega = 1.628(2)$ and $\varepsilon = 1.538(2)$ measured in white light. It is pleochroic: *O* yellow, *E* colorless; *O* > *E*. The Gladstone-Dale relationship (Mandarino 1981) was calculated; $1 - (K_p/K_c) = -0.001$ (superior) based on the ideal formula and -0.028 (excellent) based on the empirical formula, in both cases using $k(\text{UO}_3) = 0.134$ (Larsen 1921).

4. Chemical composition

Chemical analyses (6) were performed using a JEOL JXA-iHP200F electron microprobe (Caltech), operating in wavelength dispersive spectroscopy (WDS) mode and using Probe for EPMA software. Analytical conditions were 15 kV accelerating voltage, 5 nA beam current and 10 μm beam diameter. Analyses were processed with the CITZAF correction procedure (Armstrong 1995). Szilagyiiite contains major Ca, Na, Se, U, C, F, O, and H. No other elements were detected. Szilagyiiite was strongly altered under the analysis beam, leading to the low average analytical total. Analytical data are given in Tab. 1 with normalized values.

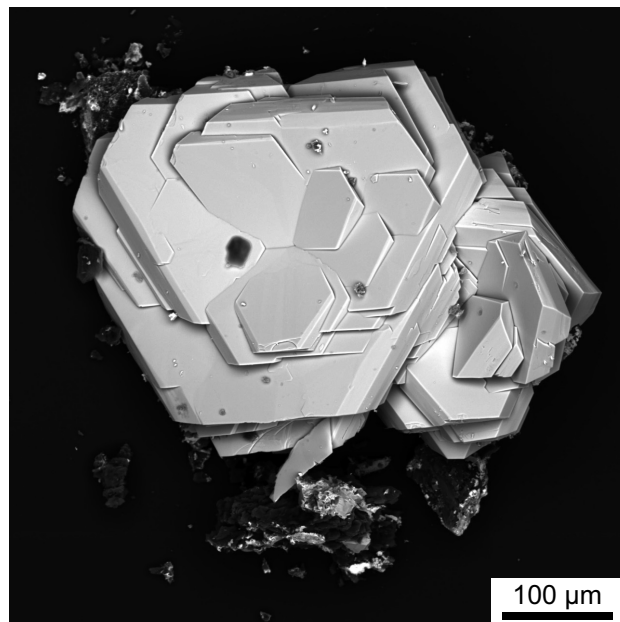


Fig. 2 Back-scattered electron image of a szilagyiiite aggregate, with matrix coated by white $[\text{Mg}(\text{H}_2\text{O})_6](\text{SeO}_3)$.

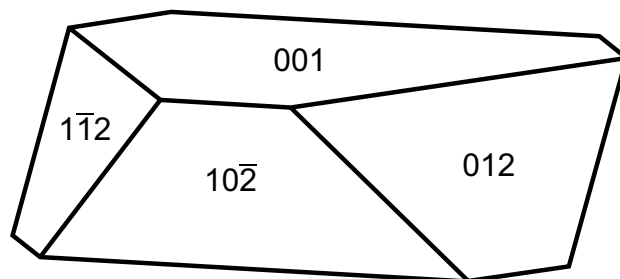


Fig. 3 Crystal drawing of szilagyiiite, clinographic projection.

Because insufficient material was available for a direct determination of CO_2 and H_2O , they were calculated based upon the structure determination ($C=3$) with H for charge balance ($21 \text{ O} + \text{F}$ and $U=1$). The empirical formula, calculated on the basis of $21 \text{ O} + \text{F}$ and $U=1$ apfu, is $\text{Na}_{0.76}\text{Ca}_{3.11}(\text{UO}_2)(\text{CO}_3)_3(\text{Se}_{1.16}\text{O}_3)\text{F}_{0.82}\text{O}_{20.18}\text{H}_{13.19}$. The simplified formula is $\text{NaCa}_3(\text{UO}_2)(\text{CO}_3)_3(\text{SeO}_3)(\text{F},\text{OH})$.

Tab. 1 Chemical composition of szilagyiiite.

Constituent	Mean	Range	S.D.	Standard	Normalized	Ideal
UO_3	30.36	30.15–30.9	0.29	UO_{2+x}	32.29	33.77
CaO	18.54	18.26–19.07	0.30	Anorthite	19.72	19.85
Na_2O	2.49	2.06–3.25	0.43	Albite	2.64	3.66
SeO_2	13.66	13.44–13.86	0.17	Se-metal	14.52	13.09
CO_2^*	14.02	–	–	–	14.91	15.58
F	1.66	1.61–1.84	0.17	F-mica	1.76	2.24
H_2O^{**}	12.61	–	–	–	13.41	12.76
F=O	–0.70	–	–	–	–0.75	–0.94
Total	94.03				100.00	100.00

*Calculated based on the structure

**Based on charge balance

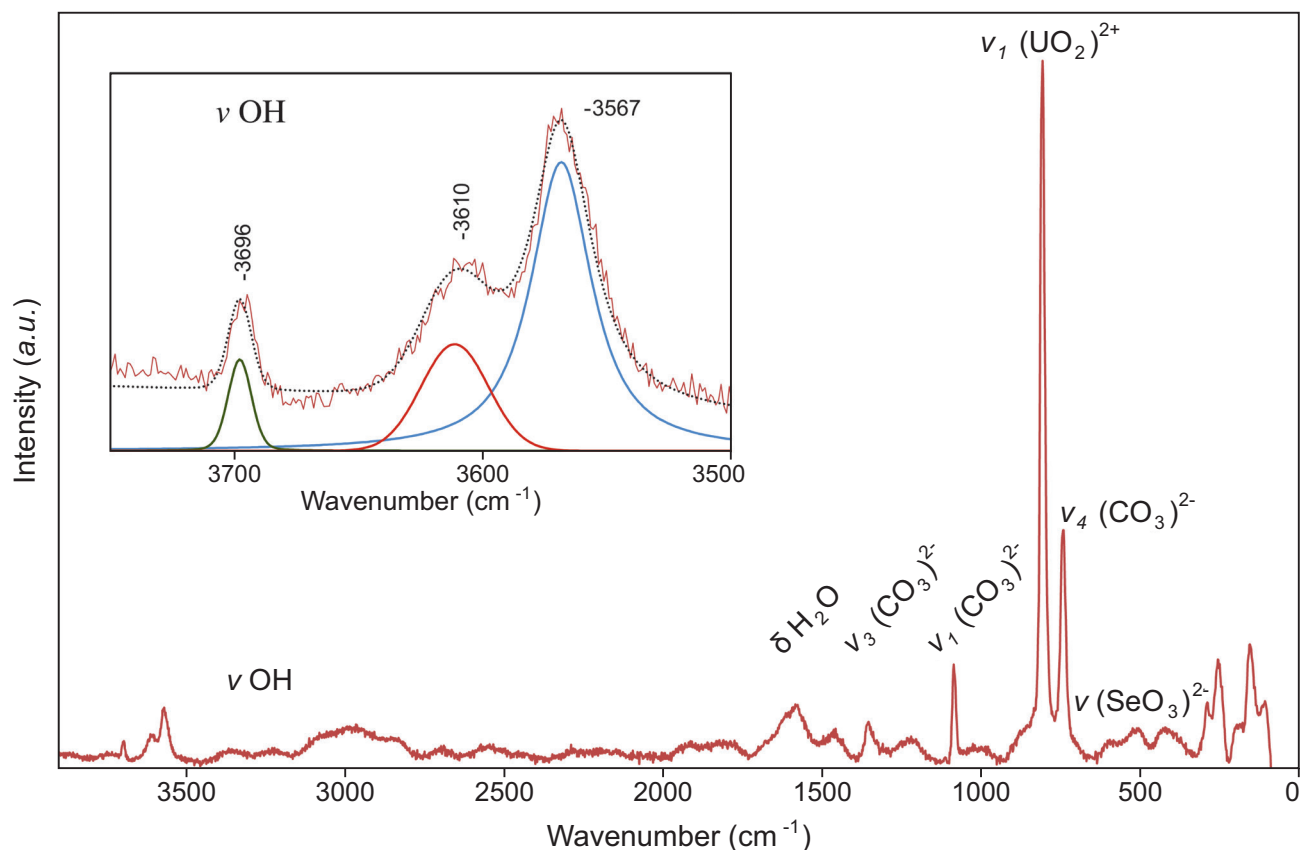


Fig. 4 Raman spectrum of szilagyite from 4000 to 90 cm^{-1} , with inset containing fitted OH region.

$(\text{H}_2\text{O})_6$. The ideal formula is $\text{NaCa}_3(\text{UO}_2)(\text{CO}_3)_3(\text{SeO}_3)\text{F}(\text{H}_2\text{O})_6$, which requires CaO 19.85, Na_2O 3.66, SeO_2 13.09, UO_3 33.77, CO_2 15.58, F 2.24 (F=O -0.94), H_2O 12.76, total 100 wt. %.

5. Raman Spectroscopy

The Raman spectrum of szilagyite was recorded using a Horiba XploRA PLUS and $100\times$ (0.9 NA) objective. The spectrum from 4000 to 60 cm^{-1} obtained using a 532 nm diode laser, 100 μm slit, and 1800 gr/mm diffraction grating is shown in Figs 4, 5. The spectrum consists of 20 accumulations, at 10 seconds per scan, and a laser power of 2 mW. We observed no laser damage or thermal effects during the measurement. All band maxima given below were derived from freely refined pseudo-Voigt peak fit-

ting after cubic spline background subtraction in Fityk 1.3.1 (Wojdyr 2010).

Multiple distinct bands between ~ 3700 – 3000 cm^{-1} arise from stretching vibrations of hydrogen-bonded F/OH and H_2O groups. The empirical correlation of Libowitzky (1999) provides O–H \cdots O hydrogen bond lengths between 3.2 and 2.7 Å, which is consistent with lengths measured in the crystal structure (Tab. 2). The FWHM of fitted band centers in this region are characterized as follows: 3696, 3610, 3567 (sharp); 3240, 3352, 2972 (ν broad). Several weak broad bands observed in the 2800–2300 cm^{-1} range are likely artifacts. While typically only observable in FTIR spectra, two very broad but moderately intense bands centered at 1601 and 1580 cm^{-1} are assigned to the (δ) bending vibration of H_2O groups.

Providing accurate assignments for bands in the region < 1500 cm^{-1} is complicated due to overlap of ν_3 (CO_3) $^{2-}$ antisymmetric stretching vibrations, U–O/OH $_{\text{eq}}$, and stretching modes of (SeO_3) $^{2-}$, which in other uranyl-selenite minerals are observed at 1379, 1344, and 1250 cm^{-1} . Thus, the weak and broad unassigned bands observed at ~ 1220 and ~ 1000 may belong to one of these modes.

Tab. 2 Hydrogen bond metrics.

Hydrogen bonds	DH	DA	HA	$\angle\text{DHA}$
OH1/F–H1 \cdots O1	0.84(4)	2.66(5)	3.506(13)	180
OH1–H1 \cdots Ow1	0.84(4)	2.475(17)	2.880(7)	110.6(10)
Ow1–H1a \cdots O1	0.80(4)	2.23(6)	2.932(9)	147(8)
Ow1–H1b \cdots O6 ¹⁶	0.82(4)	1.88(5)	2.658(7)	159(9)
Ow2–H2a \cdots Ow1 ¹²	0.79(4)	2.17(4)	2.952(8)	172(9)
Ow2–H2b \cdots O6	0.80(4)	2.48(8)	2.948(8)	119(8)

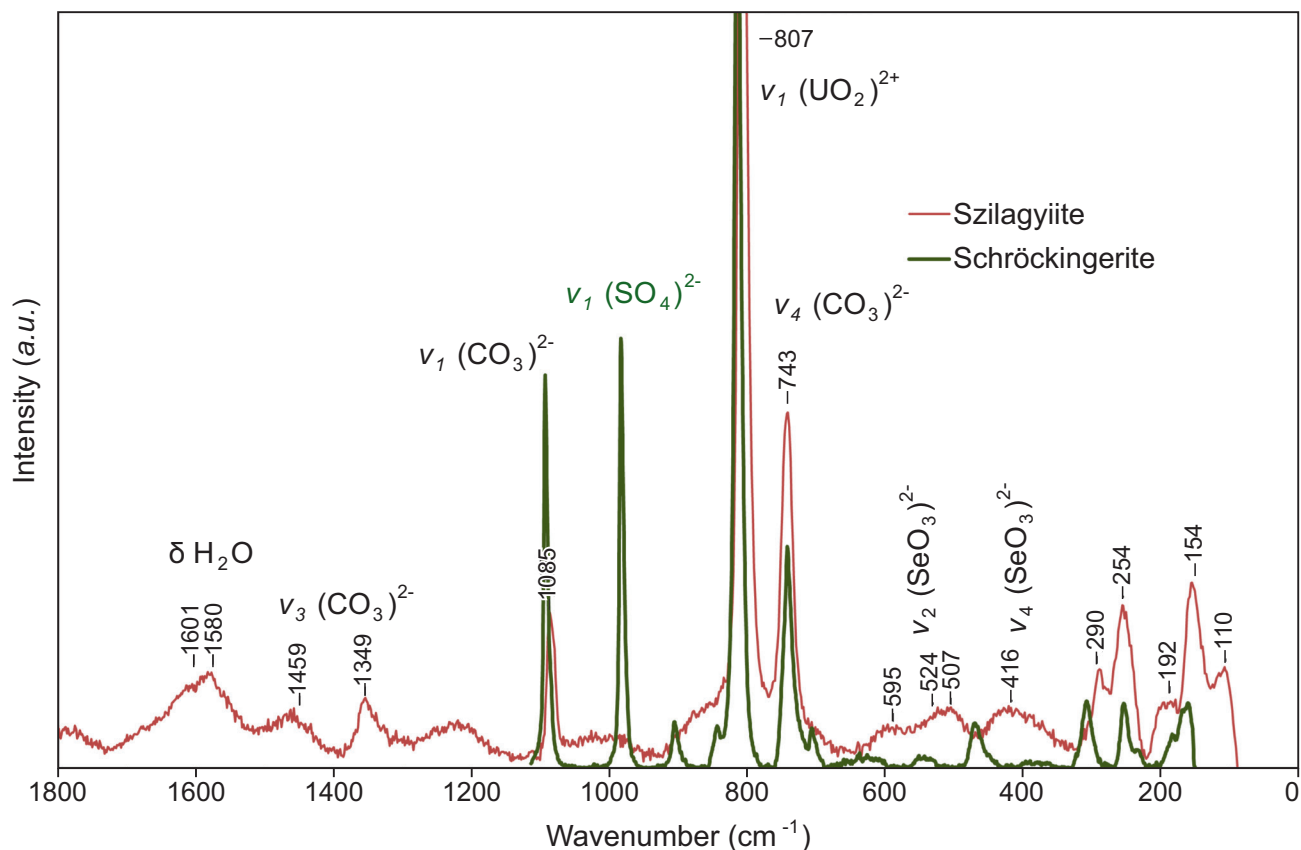


Fig. 5 Raman spectrum of szilagyite compared to schröckingerite from 1800 to 90 cm^{-1} .

The weak bands between ~ 1450 and 1300 cm^{-1} belong to the $\nu_3 (\text{CO}_3)^{2-}$ antisymmetric stretching vibrations of the $(\text{CO}_3)^{2-}$ units, with fitted centers at 1459 and 1349 cm^{-1} . The single strong band at 1085 cm^{-1} is assigned to the $\nu_1 (\text{CO}_3)^{2-}$ symmetric stretching vibration of the lone C1 site (Koglin et al. 1979; Anderson et al. 1980; Čejka 1999 and 2005). Likewise, an isolated band at 743 cm^{-1} is assigned to the $\nu_4 (\delta) (\text{CO}_3)^{2-}$ in-plane bending vibration, but this band likely overlaps with Se–O modes.

For example, in the lead uranyl selenite mineral borzeckite, a medium intensity band at 729 cm^{-1} was assigned to the antisymmetric $\nu_3 (\text{SeO}_3)^{2-}$ stretching mode of the selenite groups (Suda et al. 2022). Two additional weak bands observed at 526 and 480 cm^{-1} in borzeckite were assigned to the $\nu_2 (\text{SeO}_3)^{2-}$ bending mode. In the Raman spectrum of szilagyite, bands in this re-

gion are very poorly resolved, occurring as weak and composite peaks that are too broad to fit reliably. Their local maxima are positioned ~ 507 , 524 , and 595 cm^{-1} . In

Tab. 3 Selected bond distances (Å) for szilagyite.

Ca1–O3 ³	2.457(5)	U1–O1	1.803(11)	Se1–O6	1.698(5)
Ca1–O4	2.386(5)	U1–O2	1.776(13)	Se1–O6 ²	1.698(5)
Ca1–O5 ²	2.406(5)	U1–O3 ¹⁶	2.435(5)	Se1–O6 ³	1.698(5)
Ca1–O6	2.518(5)	U1–O3 ¹⁷	2.435(5)	<Se–O>	1.698
Ca1–O6 ³	2.676(6)	U1–O3 ¹⁸	2.435(5)		
Ca1–F/OH	2.305(3)	U1–O4 ¹⁶	2.409(5)	C1–O3	1.301(7)
Ca1–OW1	2.508(6)	U1–O4 ¹⁷	2.409(5)	C1–O4	1.287(7)
Ca1–OW2	2.447(7)	U1–O4 ¹⁸	2.409(5)	C1–O5	1.249(7)
<Ca–O/F>	2.463	<U–O _{yl} >	1.79	<C–O>	1.279
		<U–O _{eq} >	2.422		
Na1–O2 ¹³	2.548(14)				
Na1–O5	2.357(5)				
Na1–O5 ²	2.357(5)				
Na1–O5 ³	2.357(5)				
Na1–OW2 ¹	2.899(9)				
Na1–OW2 ²	2.899(9)				
Na1–OW2 ³	2.899(9)				
<Na–O>	2.617				

Symmetry transformations used to generate equivalent atoms: (1) x, y, z ; (2) $-y, x-y, z$; (3) $-x+y, -x, z$; (13) $'x+\frac{1}{2}, y+\frac{2}{3}, z+\frac{2}{3}$ '; (14) $-y+\frac{1}{2}, x-y+\frac{2}{3}, z+\frac{2}{3}$; (16) $'-y+\frac{1}{2}, -x+\frac{2}{3}, z+7/6$ '; (17) $'-x+y+\frac{1}{2}, y+\frac{2}{3}, z+7/6$ '; (18) $'x+\frac{1}{2}, x-y+\frac{2}{3}, z+7/6$ '.

borzeckiiite, a moderately intense band at 436 and very weak band at 360 cm^{-1} belong to ν_4 (SeO_3) $^{2-}$ bending modes. Again, in szilagyiiite, a very broad band from ~ 370 – 440 cm^{-1} , with ~ 416 cm^{-1} centroid may correlate with this assignment. The bands at 290 and 254 cm^{-1} are likely attributable to ν_2 (δ) (UO_2) $^{2+}$ bending vibrations and those at 192, 154, and ~ 110 cm^{-1} to phonon modes.

The strongest band occurring at 807 cm^{-1} belongs to the ν_1 (UO_2) $^{2+}$ symmetric stretching vibration. Bartlett and Cooney (1989) derived an empirical relationship to estimate U–O_{yl} bond lengths from this band position, which gives 1.78 Å (832 cm^{-1}), on par with U–O_{yl} bond lengths in the crystal structure (Tab. 3). Activation of the Raman-forbidden ν_3 (UO_2) $^{2+}$ antisymmetric stretch was not ob-

served, as the O_{yl}–U–O_{yl} dihedral angle is constrained to 180° by symmetry, though it may be present as the weak and broadly shouldering intensity from ~ 900 – 850 cm^{-1} .

6. X-ray crystallography and structure determination

6.1. Powder diffraction

X-ray powder diffraction data were recorded using a Rigaku R-Axis Rapid II curved imaging plate microdiffractometer with monochromated MoK α radiation.

A Gandolphi-like motion on the ϕ and ω axes was used to randomize the sample. Observed d values and intensities were derived by profile fitting using JADE Pro software (Materials Data, Inc., Livermore, CA, USA). Data are given in Tab. 4. Unit cell parameters refined from the powder data using JADE Pro with whole pattern fitting are $a = 9.663(3)$ Å, $c = 33.457(12)$ Å and $V = 2706.9(19)$ Å 3 .

6.2. Single-crystal X-ray diffraction and structure solution

A tabular crystal fragment with clean extinction under cross-polarized light was used for the experiment. Data were collected at room temperature using MoK α X-rays from an Incoatec I μ S2.0 microfocus source and Photon III CPAD detector mounted to a Bruker Apex II three-circle diffractometer. The APEX4 software package was used for processing collected diffraction data, including indexing, integration, scaling and corrections for background, polarization, and Lorentz effects. A multi-scan semi-empirical absorption correction was made using SADABS (Krause et al. 2015) and an initial model in the space group $R3c$ was found using the intrinsic-phasing method SHELXT (Sheldrick 2015b). SHELXL-2018 (Sheldrick 2015a) was used for the refinement and all atoms including H were located

Tab. 4 Powder X-ray data (d in Å) for szilagyiiite. Only $I \geq 3$ calculated lines are listed.

I_{obs}	d_{obs}	d_{calc}	I_{calc}	hkl	I_{obs}	d_{obs}	d_{calc}	I_{calc}	hkl
26	7.503	7.479	23	0 1 2			1.773	3	4 0 10
100	5.916	5.914	100	1 0 4	35	1.744	1.744	19	2 3 8
32	5.577	5.578	39	0 0 6			1.734	14	1 4 6
58	4.836	4.827	53	1 1 0	5	1.665	1.664	5	3 1 14
11	4.068	4.056	10	2 0 2	5	1.639	1.641	6	0 1 20
77	3.744	3.741	75	0 1 8			1.553	15	1 3 16
		3.650	6	1 1 6	20	1.555	1.547	4	3 0 18
		3.146	10	2 1 1	16	1.530	1.527	14	1 4 12
33	3.125	3.105	22	1 2 2	7	1.499	1.496	7	2 3 14
60	2.960	2.956	57	2 1 4			1.479	18	1 2 20
		2.858	6	1 2 5	23	1.480	1.473	4	2 2 18
62	2.795	2.787	56	3 0 0	11	1.416	1.414	10	3 2 16
7	2.637	2.636	6	2 1 7	6	1.394	1.394	6	6 0 0
29	2.522	2.522	25	1 2 8			1.370	4	3 4 2
		2.493	4	3 0 6	11	1.363	1.357	8	3 1 20
23	2.419	2.414	22	2 2 0	9	1.342	1.339	7	5 2 0
16	2.303	2.297	14	3 1 2			1.306	8	3 4 8
20	2.234	2.235	15	1 3 4	14	1.307	1.302	5	1 4 18
		2.215	8	2 2 6	8	1.272	1.272	6	1 3 22
11	2.200	2.192	9	1 2 11	10	1.260	1.261	10	1 6 4
5	2.081	2.075	5	2 0 14	4	1.244	1.247	4	-6 0 -12
31	2.031	2.028	30	3 1 8	10	1.222	1.220	7	6 1 8
		1.996	3	2 1 13	10	1.208	1.207	9	2 2 24
13	1.976	1.971	11	3 0 12			1.192	4	3 2 22
		1.915	4	3 2 1	6	1.187	1.182	3	3 5 4
23	1.911	1.906	18	-2-3-2	11	1.151	1.149	10	6 2 4
25	1.872	1.870	21	3 2 4	8	1.122	1.125	4	6 1 14
		1.859	3	0 0 18			1.117	5	2 6 8
40	1.828	1.825	35	4 1 0	7	1.107	1.107	6	7 1 0

after several iterations. All atoms, except H, were successfully refined with anisotropic displacement parameters. Soft restraints were used on H atom distances and displacement parameters were restrained to $1.4\times$ (H1 of OH) and $1.2\times$ (disordered H of Ow1 and Ow2) that of the parent O site. Szilagyite crystals are frequently twinned, and the structure was refined as an inversion twin ($[\bar{1}00/0\bar{1}0/00\bar{1}]$; 70.8/29.2). Additional data collection and refinement details are given in Tab. 5, atom coordinates, equivalent isotropic and anisotropic displacement parameters are given in Tab. 6, selected bond distances are provided in Tab. 3, hydrogen bond metrics in Tab. 2, and a bond valence analysis is given in Tab. 7.

6.3. Description of the crystal structure

The structure of szilagyite contains one symmetrically non-equivalent site each of U, Ca, Na, Se, C, and F, with nine O and seven H sites. The structure is based on infinite sheets extending along $\{001\}$, which contain 3 major structural components: (1) distorted cubane-like $[(\text{SeO}_3)\text{Ca}_3(\text{F,OH})(\text{H}_2\text{O})_3]$ units (Fig. 6a), (2) $\text{NaO}_4(\text{H}_2\text{O})_3$

monocapped trigonal antiprisms (Fig. 6b), and (3) hexagonal bipyramidal uranyl tricarbonate cluster (UTC) units, $[\text{UO}_2(\text{CO}_3)_3]$ (Fig. 6c). The sheet topology is shown in Fig. 7a. Each UTC unit shares three of its U-

Tab. 5 Data collection and structure refinement details for szilagyite.

Diffractometer	Bruker Apex II with Photon III CPAD detector
X-ray radiation/power	MoK α ($\lambda = 0.71075$ Å)/50 kV, 0.6 mA
Temperature	296(2) K
Chemical Formula	$\text{NaUC}_3\text{SeCa}_3\text{F}_{0.80}\text{O}_{20.20}\text{H}_{12.2}$
Space group	$R3c$ (#161)
Unit cell dimensions	$a = 9.6542(9)$ Å $c = 33.465(5)$ Å
V	$2701.2(6)$ Å ³
Z	6
Density (for above formula)	3.124 g·cm ⁻³
Absorption coefficient	12.025 mm ⁻¹
$F(000)$	2376
Crystal size	$130 \times 90 \times 50$ μm
θ range	2.723 to 35.049°
Index ranges	$-15 \leq h \leq 15$, $-15 \leq k \leq 15$, $-51 \leq l \leq 52$
Reflections collected/unique	$15786/2544$; $R_{\text{int}} = 0.0477$
Reflections with $I > 4\sigma_I$	2335
Completeness to $\theta = 35.049^\circ$	96.3%
Refinement method	Full-matrix least-squares on F^2
Parameter/restraints	105/6
GoF	1.071
Final R indices [$I > 4\sigma_I$]	$R_1 = 0.0315$, $wR_2 = 0.0501$
R indices (all data)	$R_1 = 0.0363$, $wR_2 = 0.0514$
Twin law, Flack ratio(err)	$[\bar{1} 0 0 \ 0 \ \bar{1} 0 \ 0 \ 0 \ \bar{1}]$, 0.292(10)
Largest diff. peak/hole	$+1.46/-2.96$ e Å ⁻³

$$R_{\text{int}} = \Sigma |F_o^2 - F_c^2(\text{mean})| / \Sigma [F_o^2], \text{ GoF} = S = \{\Sigma [w(F_o^2 - F_c^2)^2] / (n-p)\}^{1/2}, R_1 = \Sigma ||F_o| - |F_c|| / \Sigma [F_o],$$

$$wR_2 = \{\Sigma [w(F_o^2 - F_c^2)^2] / \Sigma [w(F_o^2)^2]\}^{1/2}; w = 1/[\sigma^2(F_o^2) + (aP)^2 + bP] \text{ where } a \text{ is } 0.0033, b \text{ is } 27.6779 \text{ and } P \text{ is } [2F_c^2 + \text{Max}(F_o^2, 0)]/3$$

Tab. 6 Refined site occupancies, atomic coordinates and displacement parameters (Å²) for the structure of szilagyite.

Atoms	Occ.	x	y	z	$U_{\text{eq}}/U_{\text{iso}}$	U^{11}	U^{22}	U^{33}	U^{12}	U^{13}	U^{23}
U1	$\text{U}_{1.00}$	$\frac{2}{3}$	$\frac{1}{3}$	0.15867(2)	0.00957(7)	0.00824(7)	0.00824(7)	0.01221(16)	0	0	0.00412(4)
Se1	$\text{Se}_{1.00}$	$\frac{2}{3}$	$\frac{1}{3}$	-0.09975(3)	0.0167(3)	0.0177(2)	0.0177(2)	0.0145(8)	0	0	0.00887(12)
Ca1	$\text{Ca}_{1.00}$	0.43345(13)	0.31435(13)	-0.02353(5)	0.01113(19)	0.0080(4)	0.0078(4)	0.0170(6)	-0.0005(4)	-0.0009(4)	0.0035(4)
Na1	$\text{Ca}_{1.00}$	0	0	-0.04545(16)	0.0275(14)	0.0243(16)	0.0243(16)	0.034(5)	0	0	0.0121(8)
O1	$\text{O}_{1.00}$	$\frac{2}{3}$	$\frac{1}{3}$	0.1048(3)	0.015(2)	0.016(4)	0.016(4)	0.014(6)	0	0	0.0079(19)
O2	$\text{O}_{1.00}$	$\frac{2}{3}$	$\frac{1}{3}$	0.2117(4)	0.026(3)	0.031(5)	0.031(5)	0.017(7)	0	0	0.015(3)
O3	$\text{O}_{1.00}$	0.6217(6)	0.8457(5)	-0.00677(17)	0.0179(11)	0.0111(19)	0.0061(17)	0.038(3)	-0.0040(18)	-0.001(2)	0.0054(15)
O4	$\text{O}_{1.00}$	0.5369(6)	0.5921(5)	-0.01069(17)	0.0151(10)	0.010(2)	0.0063(19)	0.027(3)	-0.0004(17)	0.0003(19)	0.0028(16)
O5	$\text{O}_{1.00}$	0.7995(5)	0.7632(5)	-0.01542(17)	0.0180(9)	0.0111(19)	0.015(2)	0.030(3)	-0.004(2)	-0.0016(19)	0.0082(16)
O6	$\text{O}_{1.00}$	0.5118(5)	0.1783(5)	-0.07575(15)	0.0202(10)	0.017(2)	0.014(2)	0.023(3)	-0.0024(18)	0.0059(19)	0.0023(17)
C1	$\text{C}_{1.00}$	0.6589(7)	0.7343(7)	-0.0114(2)	0.0120(11)	0.009(2)	0.012(2)	0.017(3)	0.001(2)	0.002(2)	0.007(2)
OW1	$\text{O}_{1.00}$	0.4259(6)	0.3320(7)	0.05113(19)	0.0241(12)	0.014(2)	0.031(3)	0.026(3)	0.010(2)	0.002(2)	0.010(2)
OW2	$\text{O}_{1.00}$	0.2676(9)	0.2753(9)	-0.0824(2)	0.0382(16)	0.044(4)	0.059(5)	0.028(4)	-0.012(3)	-0.018(3)	0.039(3)
F/OH1	$\text{F}_{0.80}\text{O}_{0.20}$	$\frac{2}{3}$	$\frac{1}{3}$	0.0000(2)	0.0144(12)	0.0135(17)	0.0135(17)	0.016(4)	0	0	0.0067(9)
H1	$\text{H}_{0.20}$	$\frac{2}{3}$	$\frac{1}{3}$	0.0252(13)	0.022	-	-	-	-	-	-
H1A	$\text{H}_{1.00}$	0.476(10)	0.296(10)	0.061(2)	0.022	-	-	-	-	-	-
H1B	$\text{H}_{1.00}$	0.333(6)	0.270(8)	0.058(3)	0.022	-	-	-	-	-	-
H2A	$\text{H}_{1.00}$	0.226(10)	0.318(11)	-0.093(3)	0.022	-	-	-	-	-	-
H2B	$\text{H}_{1.00}$	0.290(11)	0.222(10)	-0.096(2)	0.022	-	-	-	-	-	-

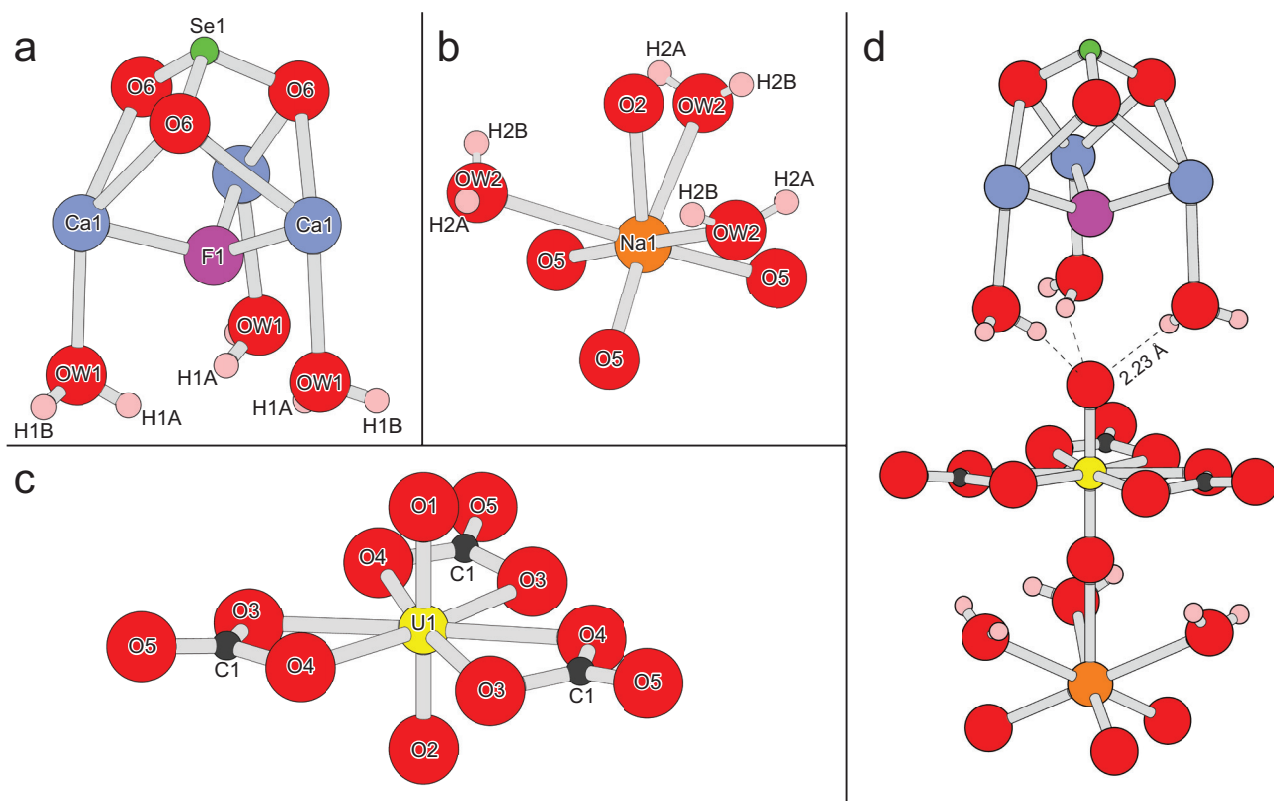


Fig. 6 Ball-and-stick models of the structural components in szilagyite, including atom labels for the: **a** – $[(\text{SeO}_3)\text{Ca}_3(\text{H}_2\text{O})_3(\text{F},\text{OH})]$; **b** – $\text{NaO}_4(\text{H}_2\text{O})_3$; and **c** – $(\text{UO}_2)(\text{CO}_3)_3$ units. **d** – shows the columnar arrangement between each unit.

O_{eq} edges with edges of irregular Ca polyhedra of the $[(\text{SeO}_3)\text{Ca}_3(\text{F},\text{OH})(\text{H}_2\text{O})_3]$ units. The three outwardly extended O^{2-} of each $(\text{CO}_3)^{2-}$ group in one UTC unit is shared with three neighboring Na polyhedra in the sheet. The sheets are cross-linked through U–O–Na bonds along *c* via the -yl O2 site (Fig. 6d). The sheets are also weakly cross-linked by hydrogen bonds between $\text{H}_2\text{O}/\text{OH}/\text{F}$ groups in the sheets and correspond to the perfect $\{001\}$ cleavage.

The U1 site has multiply bonded apical ‘yl’ oxygen atoms (O_{yl}) forming the linear uranyl cation $(\text{UO}_2)^{2+}$. The uranyl cation is coordinated six-fold equatorially by oxygen atoms of three bidentate CO_3^{2-} groups forming the hexagonal bipyramidal uranyl tricarbonate unit (UTC). The Ca1 site occurs within a cubane-like $[(\text{SeO}_3)\text{Ca}_3(\text{F},\text{OH})]$ unit, constituting one of the three major structural motifs. It is [8]-coordinated, forming an irregularly shaped polyhedron with three Ca poly-

Tab. 7 Bond valence analysis for szilagyite. Values are expressed in valence units.*

Atom	U1	Ca1	Na1	Se1	C1	Hydrogen Bonds			Σ_{an}
						Donor	vu**	H bond	
O1	1.60	–	–	–	–	OW1	0.15	$\times 3 \rightarrow$	2.04
O2	1.68	–	0.011	–	–	OW2	0.15	$\times 2 \rightarrow$	1.98
O3	1.46	0.26	–	–	1.28	–	–	–	2.01
O4	1.39 $\times 3 \downarrow$	0.31	–	–	1.32	–	–	–	2.10
O5	–	0.30	0.20 $\times 3 \downarrow$	–	1.45	–	–	–	1.95
O6	–	0.38	–	1.31 $\times 3 \downarrow$	–	OW1	0.25	–	1.94
F/OH1	–	0.255†	–	–	–	H1	–	–	0.77
OW1	–	0.23	–	–	–	OW2	0.14	–	0.37
OW2	–	0.27	0.053 $\times 3 \downarrow$	–	–	–	–	–	0.43
Σ_{cat}	6.12	1.99	0.77	3.93	4.05				

*Bond valence parameters for non-hydrogen bonds are from Gagné and Hawthorne (2015). **Bond valence parameters (D–A) for hydrogen bonds are derived from Ferraris and Ivaldi (1988). †Occupancy adjusted value (F : OH 0.8 : 0.2).

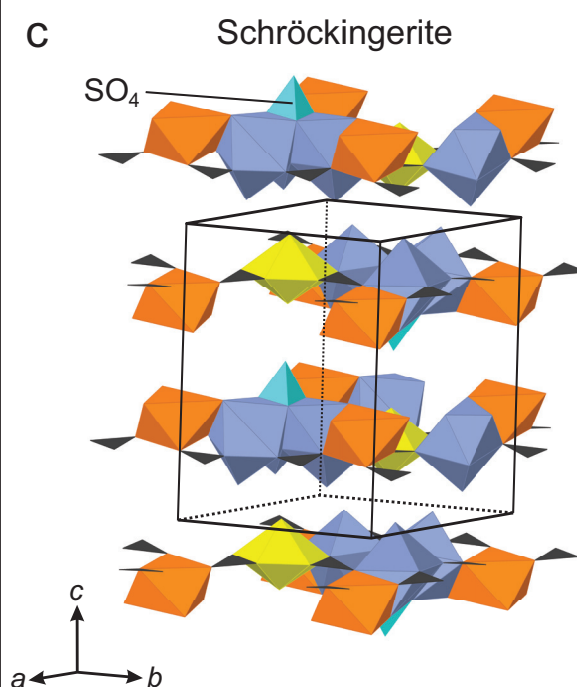
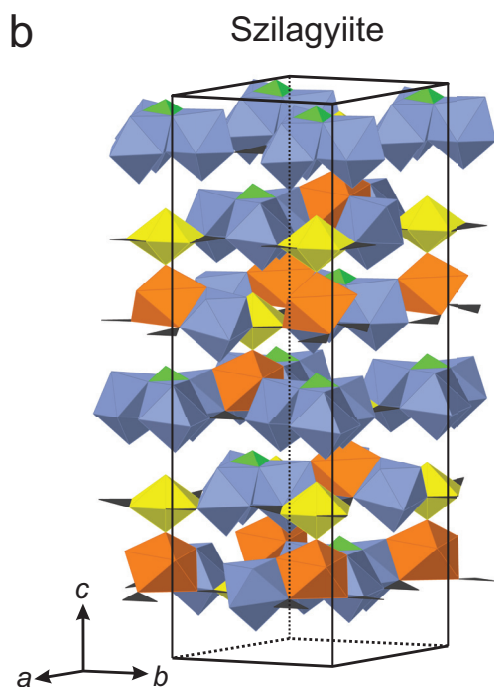
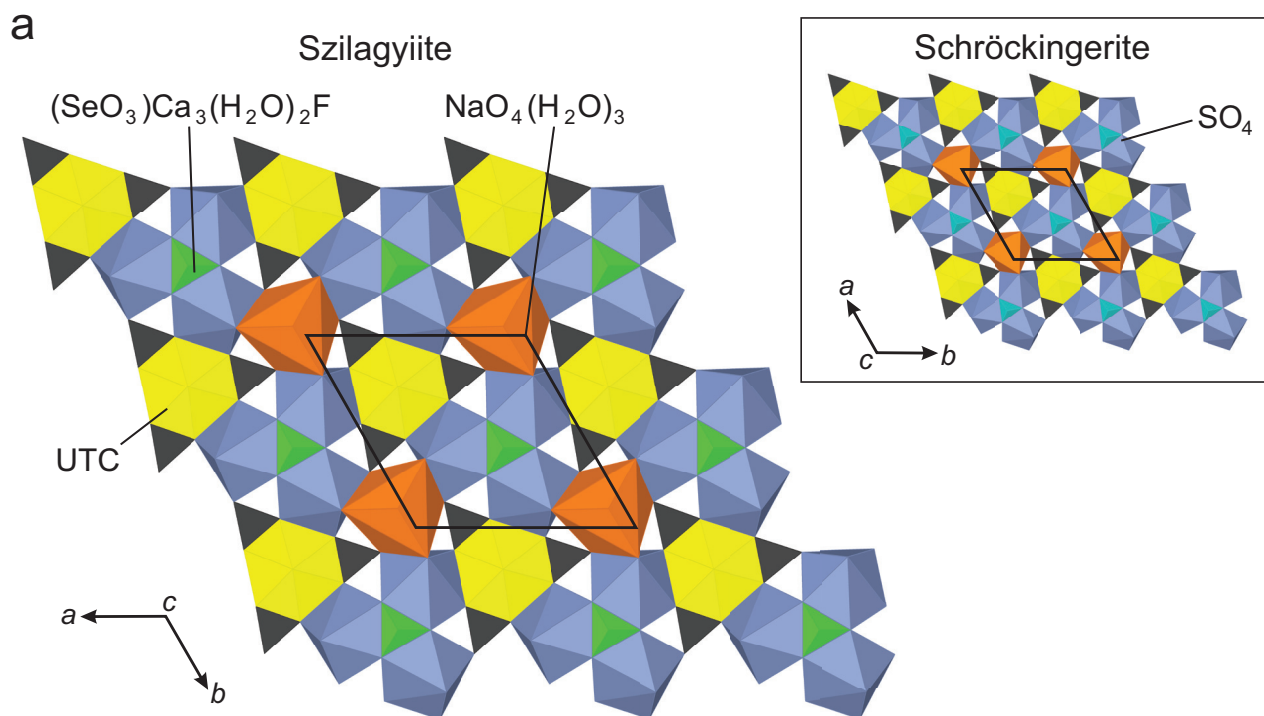


Fig. 7 Polyhedral model of the sheet topology in szilagyite (a, b) and schröckingerite (c). Unit cell outlines are shown with solid black lines. For simplicity, interlayer water molecules are not shown in schröckingerite.

hedra arranged trigonally about the Ca–F bond. The Ca–F bond measures 2.305 Å, distinctly shorter than the Ca–O bonds. In the structure of schröckingerite presented in Mereiter (1986), the Ca–F bonds measure 2.314–2.319 Å.

During the refinement of szilagyite, difference Fourier mapping located electron density located roughly ~ 1 Å from the O/F site—corresponding to a hydroxyl H atom. Based on EPMA chemistry, the site contains F:O at a ratio $\sim 0.8:0.2$, and site occupancy factors (SOF) for O (and

Tab. 8 Structural complexity (bits/u.c.) of select uranyl carbonate minerals.

Mineral	Formula	Volume	$I_{G,Total}$ (bits/u.c.)
albrechtschraufite ⁱ	$MgCa_4F_2[(UO_2)(CO_3)_3]_2(H_2O)_{17-18}$	1175	1020.28
andersonite ⁱⁱ	$Na_2Ca[(UO_2)(CO_3)_3](H_2O)_{5.333-5.6}$	6544	567.38
bayleyite ⁱⁱⁱ	$Mg_2[UO_2(CO_3)_3](H_2O)_{18}$	2624	1510.28
braunerite ^{iv}	$K_2Ca(UO_2)(CO_3)_3(H_2O)_{6-7}$	5958	2305.36
čejkaite ^v	$Na_4[(UO_2)(CO_3)_3]$	964	161.42
ewingite ^{vi}	$Mg_8Ca_8(UO_2)_{24}(CO_3)_{30}O_4(OH)_{12}(H_2O)_{138}$	59245	12684.86
leószilárdite ^{vii}	$Na_6Mg[(UO_2)(CO_3)_3]_2(H_2O)_6$	1189	179.33
liebigite ^{viii}	$Ca_2(UO_2)(CO_3)_3(H_2O)_{11}$	4022	567.53
línekite ^{ix}	$K_2Ca_3[(UO_2)(CO_3)_3]_2(H_2O)_8$	5622	2140.57
markeyite ^x	$Ca_9(UO_2)_4(CO_3)_{13}(H_2O)_{28}$	3357	1115.06
natromarkeyite ^{xi}	$Na_2Ca_8(UO_2)_4(CO_3)_{13}(H_2O)_{27}$	3347	1685.99
paddlewheelite ^{xii}	$MgCa_5Cu_2(UO_2)_4(CO_3)_{12}(H_2O)_{33}$	7306	3386.93
paramarkeyite ^{xiii}	$Ca_2(UO_2)(CO_3)_3(H_2O)_5$	5676	2400.67
pseudomarkeyite ^{xiv}	$Ca_8(UO_2)_4(CO_3)_{12}(H_2O)_{21}$	2882	1004.68
roubaultite ^{xv}	$Cu_2(UO_2)_3(CO_3)_2O_2(OH)_2(H_2O)_4$	421	156.75
rutherfordine ^{xvi}	$UO_2(CO_3)$	193	15.65
schröckingerite ^{xvii}	$NaCa_3(UO_2)(CO_3)_3(SO_4)F(H_2O)_{10}$	1151	578.59
swartzite ^{xviii}	$CaMg[(UO_2)(CO_3)_3](H_2O)_{12}$	1023	527.16
szilagyiiite^{xiv}	$NaCa_3(UO_2)(CO_3)_3(SeO_3)F(H_2O)_6$	2701	417.11

References: ⁱMereiter (2013); ⁱⁱCoda et al. (1981); ⁱⁱⁱMayer and Mereiter (1986); ^{iv}Plášil et al. (2016); ^vPlášil et al. (2013); ^{vi}Olds et al. (2017a); ^{vii}Olds et al. (2017b); ^{viii}Mereiter (1982); ^{ix}Plášil et al. (2017); ^xKampf et al. (2018); ^{xi}Kampf et al. (2020); ^{xii}Olds et al. (2018); ^{xiii}Kampf et al. (2022b); ^{xiv}Kampf et al. (2020); ^{xv}Ginderow and Cesbron (1985); ^{xvi}Finch et al. (1999); ^{xvii}Mereiter (1986a); ^{xviii}Mereiter (1986b); ^{xiv}This work.

its H) were set accordingly. The $[(SeO_3)Ca_3(F,OH)]$ unit is directly analogous to the $[(SO_4)Ca_3(F,OH)]$ unit found in schröckingerite (Fig. 7c). The Se^{4+} lone pair projects towards Na along *c* to complete a pseudo-tetrahedral arrangement for SeO_3 . Structures with SeO_3 (and TeO_3) trigonal pyramids (e.g., chalcocite, $CuSeO_3 \cdot 2H_2O$) feature “void” spaces that accommodate the SeO_3 lone pair (Robinson et al. 1992). The Na1 site is [7]-coordinated: three bonds to O shared by three symmetrically equivalent CO_3 groups (2.358 Å), three bonds to O of H_2O groups (2.896 Å), and one bond to an O atom shared in the neighboring sheet (2.550 Å). Based on this, we propose the structural formula: $Na[(UO_2)(CO_3)_3][(SeO_3)Ca_3(H_2O)_6(F,OH)]$.

6.4. Hydrogen bonds – H_2O and F/OH as bond strength transformers

As described by Hawthorne (1992), the crystal structure of most oxysalt minerals is best thought of as a two-component system. The first, a structural unit, bearing strong bonds (>0.3 v.u.) and (usually) a negative charge, and second, the interstitial complex with a net positive charge, containing weakly bonded constituents such as low valence cations and anions, and H_2O . In szilagyiiite, the structural unit consists of tightly interlocked sheets of $[UO_2(CO_3)_3]^{4-}$, and $[(SeO_3)Ca_3(F,OH)]^{3+}$ units. The interlayer consists of just a thin layer of H_2O groups and weakly bonded Na^+ that spans roughly ~ 4 Å wide. Hydrogen bonds occur between the two H_2O groups Ow1 and

Ow2, and partially occupied hydroxyl OH1/F1 (Tab. 2). Together, Ow1 and Ow2 are fully occupied, constituting 6 H_2O *pfu*, and it can apparently not accommodate more; however, the mineral appears relatively stable to dehydration, except under vacuum.

The hydrogen atoms of Ow1 (H1a and H1b) form strong hydrogen bonds with O6 of the SeO_3 groups and the uranyl O1. The H1 site of F1/OH1 (0.2 OH *pfu*) is shielded within a pocket of the three Ow1 sites, and apparently does not participate in hydrogen bonding with the uranyl oxygen O1 ($D-A \sim 3.5$ Å); however, the metrics are still included in Tab. 2 for reference. Ow1 also accepts H-bonds from Ow2 via H2a. The role of Ow1 in this case is as a bond-valence transformer, shuttling valence from Ca-trimers in one sheet through its hydrogen bonds to the next sheet via adjacent O_{y1} and O of SeO_3 , the two strongest H-bonds in the structure. Conversely, Ow2 acts as a non-transformer bonded to two cations (“ H_2O_e ”), Ca and Na. The hydrogen sites belonging to Ow2 are ordered, with H2a donating to Ow1, and H2b to O3 and/or O6. Though the refined positions of H2a and H2b place Ow2–O2 interactions at an angle precluding hydrogen bonding, it is clear from Tab. 7 that O2 requires at least 2 H-bonds ($1.69 + 0.15 + 0.15$). The uranyl site O1 accepts three hydrogen bonds – one from each H1A.

6.5. Complexity

As determined by the method introduced by Krivovichev (2012) and calculated using ToposPro (Blatov et

al. 2014), the structural complexity of szilagyite is high at 417.11 bits/u.c. (Tab. 8). Despite its large unit cell volume, it has a low complexity relative to other uranyl carbonates, a function of its high symmetry and lower water content, like the closely related schröckingerite, measuring 578.59 bits/u.c.

6.6. Relationship to other species

Szilagyite is a member of the uranyl carbonates with U:C = 1:3, Nickel-Strunz class 05.ED. Szilagyite represents a unique combination of elements among known minerals; there are just 8 minerals with essential U and Se at the time of writing, and interestingly, each contain selenite (SeO_3)²⁻; there are no known uranyl minerals bearing selenate SeO_4 . Szilagyite is both structurally and chemically related to the uranyl carbonate-sulfate mineral schröckingerite, $\text{NaCa}_3(\text{UO}_2)(\text{CO}_3)_3(\text{SO}_4)\cdot 10\text{H}_2\text{O}$, and bears some chemical similarity to albrechtschraufite, $\text{Ca}_4\text{Mg}(\text{UO}_2)_2(\text{CO}_3)_6\text{F}_2\cdot 17\text{--}18\text{H}_2\text{O}$, though shares no related structural elements beyond the UTC units.

Szilagyite and schröckingerite share a closely related sheet topology (swapping SeO_3 for SO_4) but differ in the stacking arrangement, as well as the number and types of bonds that hold them together, which is largely a function of the extra H_2O groups in schröckingerite, and its much lower symmetry (*P*-1). This difference in stacking arrangement (Fig 6b, c) and H_2O content is reflected in the *c* parameters of each mineral (33.465 Å in szilagyite; 14.391 Å in schröckingerite). In schröckingerite, the “extra” protruding O site of the sulfate groups requires significantly more bond valence, which is provided by the additional interlayer H_2O groups and a stacking arrangement that more closely “nests” sulfate groups from two mirrored sheets together. In schröckingerite, strong trigonal pseudosymmetry is derived from many heavy atoms present on pseudo-threefold axes. In szilagyite, sheets stack on top of one another, where all selenite polyhedra point in the same direction. One could then speculate that the presence of SeO_3 in szilagyite, having only nebulous lone-pairs and lacking such strong interactions to next-neighbor sheets as in schröckingerite, leads to crystallization in the acentric polar space group, the pronounced subparallel growth, and ubiquitous twinning.

Acknowledgements. We thank Dr. Jiří Sejkora and two anonymous reviewers for comments that significantly improved the quality of this manuscript. TAO and CE were supported by the Henry L. Hillman Foundation. A portion of this study was funded by the John Jago Trelawney Endowment to the Mineral Sciences Department of the Natural History Museum of Los Angeles County. The EPMA was carried out at the Caltech GPS Division

Analytical Facility, which is supported, in part, by NSF Grant EAR-2117942.

References

- ANDERSON A, CHIEH C, IRISH DE, TONG JP (1980) An X-ray crystallographic, Raman, and infrared spectral study of crystalline potassium uranyl carbonate, $\text{K}_4\text{UO}_2(\text{CO}_3)_3$. *Can J Chem* 58(16): 1651–1658
- ARMSTRONG JT (1995) CITZAF: a package of correction programs for the quantitative electron X-ray analysis of thick polished materials, thin films, and particles. *Microbeam Anal* 4: 177–200
- BARTLETT JR, COONEY RP (1989) On the determination of uranium-oxygen bond lengths in dioxouranium(VI) compounds by Raman spectroscopy. *J Molecul Struct* 193: 295–300
- BLATOV VA, SHEVCHENKO AP, PROSERPIO DM (2014) Applied topological analysis of crystal structures with the program package ToposPro. *Cryst Growth Des* 14: 3576–3586
- ČEJKA J (1999) Infrared spectroscopy and thermal analysis of the uranyl minerals. In: RIBBE PH, BURNS PC, FINCH R (eds) Uranium: Mineralogy Geochemistry and the Environment. *Mineral Soc Amer Rev Mineral* 38: pp 521–622
- ČEJKA J (2005) Vibrational spectroscopy of the uranyl minerals – infrared and Raman spectra of the uranyl minerals. II. Uranyl carbonates. *Bull mineral-petrolog Odd Nár Muz (Praha)* 13: 62–72.
- CODA A, DELLA GIUSTA A, TAZZOLI V (1981) The Structure of Synthetic Andersonite, $\text{Na}_2\text{Ca}[\text{UO}_2(\text{CO}_3)_3]\cdot x\text{H}_2\text{O}$ ($x \sim 5.6$) *Acta Cryst B*37: 1496–1500
- FINCH RJ, COOPER MA, HAWTHORNE FC, EWING RC (1999): Refinement of the crystal structure of rutherfordine. *Canad Mineral* 37: 929–938
- FERRARIS G, IVALDI G (1988) Bond valence vs bond length in $\text{O}\cdots\text{O}$ hydrogen bonds. *Acta Crystallogr B*44: 341–344
- GAGNÉ OC, HAWTHORNE FC (2015) Comprehensive derivation of bond-valence parameters for ion pairs involving oxygen. *Acta Crystallogr B*71: 562–578
- GINDEROW D, CESBRON F (1985) The structure of roubaultite, $\text{Cu}_2(\text{UO}_2)_3(\text{CO}_3)_2\text{O}_2(\text{OH})_2\cdot 4\text{H}_2\text{O}$. *Acta Cryst C*41: 654–657
- GORMAN-LEWIS D, BURNS PC, FEIN JB (2008) Review of uranyl mineral solubility measurements. *J Chem Thermodyn* 40: 335–352
- HAWTHORNE FC (1992) The role of OH and H_2O in oxide and oxysalt minerals. *Z Kristallogr* 201: 183–206
- KAMPF AR, PLÁŠIL J, KASATKIN AV, MARTY J, ČEJKA J (2018) Markeyite, a new calcium uranyl carbonate mineral from the Markey mine, San Juan County, Utah, USA. *Mineral Mag* 82: 1089–1100

- KAMPF AR, HUGHES JM, NASH BP, MARTY J (2019) Bicapite, $\text{KNa}_2\text{Mg}_2(\text{H}_2\text{PV}^{5+}_{14}\text{O}_{42})\cdot 25\text{H}_2\text{O}$, a new polyoxometalate mineral with a bicapped Keggin anion from the Pickett Corral mine, Montrose County, Colorado, USA. *Am Mineral* 104: 1851–1856
- KAMPF AR, OLDS TA, PLÁŠIL J, BURNS PC, MARTY J (2020) Natromarkeyite and pseudomarkeyite, two new calcium uranyl carbonate minerals from the Markey mine, San Juan County, Utah, USA. *Mineral Mag* 84: 753–765
- KAMPF AR, HUGHES JM, MA C, MARTY J (2022a) Pseudodickthomssenite, $\text{Mg}(\text{VO}_3)_2\cdot 8\text{H}_2\text{O}$, a New Mineral from the Pickett Corral Mine, Bull Canyon, Montrose County, Colorado, USA. *Canad Mineral* 60: 797–804
- KAMPF AR, OLDS TA, PLÁŠIL J, BURNS PC, ŠKODA R, MARTY J (2022b) Paramarkeyite, a new calcium–uranyl–carbonate mineral from the Markey mine, San Juan County, Utah, USA. *Mineral Mag* 86: 27–36
- KOGLIN E, SCHENK HJ, SCHWOCHAU K (1979) Vibrational and low temperature optical spectra of the uranyl tricarbonate complex $[\text{UO}_2(\text{CO}_3)_3]^{4-}$. *Spectrochim Acta* 35A: 641–647
- KRAUSE L, HERBST-IRMER R, SHELDRIK GM, STALKE D (2015). Comparison of silver and molybdenum microfocus X-ray sources for single-crystal structure determination. *J Appl Cryst*: 48, 3–10
- KRIVOVICHEV SV (2012) Topological complexity of crystal structures: quantitative approach. *Acta Crystallogr A* 68: 393–398
- LARSEN ES (1921) The microscopic determination of the nonopaque minerals. U.S. Geological Survey, 679, pp 1–279
- LIBOWITZKY E (1999) Correlation of O–H stretching frequencies and O–H···O hydrogen bond lengths in minerals. *Monatsh Chem* 130: 1047–1059
- MANDARINO JA (1981) The Gladstone – Dale relationship: Part IV. The compatibility concept and its application. *Canad Mineral* 19: 441–450
- MAYER H, MEREITER K (1986) Synthetic bayleyite, $\text{Mg}_2\text{UO}_2(\text{CO}_3)_3\cdot 18\text{H}_2\text{O}$ – thermochemistry, crystallography and crystal-structure. *Tschermaks Mineral Petrogr Mitt* 35: 133–146
- MEREITER K (1982) The crystal-structure of liebigite, $\text{Ca}_2\text{UO}_2(\text{CO}_3)_3\cdot \sim 11\text{H}_2\text{O}$. *Tschermaks Mineral Petrogr Mitt* 30: 277–288
- MEREITER K (1986a) Crystal-structure and crystallographic properties of a schröckingerite from Joachimsthal. *Tschermaks Mineral Petrogr Mitt* 35: 1–18
- MEREITER K (1986b) Synthetic swartzite, $\text{CaMgUO}_2(\text{CO}_3)_3\cdot 12\text{H}_2\text{O}$, and its strontium analog, $\text{SrMgUO}_2(\text{CO}_3)_3\cdot 12\text{H}_2\text{O}$ – crystallography and crystal-structures: *Neu Jb Mineral, Mh* 11: 481–492
- MEREITER K (2013) Description and crystal structure of albrechtschraufite, $\text{MgCa}_4\text{F}_2[(\text{UO}_2)(\text{CO}_3)_3]_2(\text{H}_2\text{O})_{17-18}$. *Mineral Petrol* 107: 179–188
- OLDS TA, PLÁŠIL J, KAMPF AR, BURNS PC, SIMONETTI A, SADERGASKI LR (2017a) Ewingite: Earth’s most complex mineral. *Geology* 45: 1007–1010
- OLDS TA, SADERGASKI L, PLÁŠIL J, KAMPF AR, BURNS PC, STEELE IM, MARTY J (2017b) Leószilárdite, the first Na,Mg-containing uranyl carbonate from the Markey Mine, San Juan County, Utah, USA. *Mineral Mag* 81: 1039–1050
- OLDS TA, PLÁŠIL J, KAMPF AR, DAL BO F, BURNS PC (2018) Paddlewheelite, a New Uranyl Carbonate from the Jáchymov District, Bohemia, Czech Republic. *Minerals* 8: 511
- OLDS TA, KAMPF AR, HUGHES JM, ADAMS PM, MARTY J (2024) Trebiskyite, the First Titanium-Decavanadate Mineral. *Can J Mineral Petrol* 62: 117–132
- PLÁŠIL J, FEJFAROVÁ K, DUŠEK M, ŠKODA R, ROHLÍČEK J (2013) Revision of the symmetry and the crystal structure of čejkaite, $\text{Na}_4(\text{UO}_2)(\text{CO}_3)_3$. *Am Mineral* 98: 549–553
- PLÁŠIL J, MEREITER K, KAMPF AR, HLOUŠEK J, ŠKODA R, ČEJKA J, NĚMEC I, EDEROVÁ J (2016) Braunerite, IMA 2015-123, CNMNC Newsletter No. 31, June 2016. *Mineral Mag* 80: 691–697
- PLÁŠIL J, ČEJKA J, SEJKORA J, HLOUŠEK J, ŠKODA R, NOVÁK M, DUŠEK M, ČISAŘOVÁ I, NĚMEC I, EDEROVÁ J (2017) Línekite, $\text{K}_2\text{Ca}_3[(\text{UO}_2)(\text{CO}_3)_3]_2\cdot 8\text{H}_2\text{O}$, a new uranyl carbonate mineral from Jáchymov, Czech Republic. *J Geosci* 62: 201–213
- ROBINSON PD, SEN GUPTA PK, SWIHART GH, HOUK L (1992) Crystal structure, H positions, and the Se lone pair of synthetic chalcomenite, $\text{Cu}(\text{H}_2\text{O})_2[\text{SeO}_3]$. *Am Mineral* 77: 834–838
- SHELDRIK GM (2015a) Crystal Structure refinement with SHELX. *Acta Cryst C* 71: 3–8
- SHELDRIK G.M. (2015b) SHELXT – Integrated space-group and crystal-structure determination. *Acta Crystallogr A* 71: 3–8
- SIMANDL GJ, PARADIS S (2022) Vanadium as a critical material: economic geology with emphasis on market and the main deposit types. *Appl Earth Sci* 131, 218–236
- SIUDA R, KRUSZEWSKI Ł, OLDS TA (2022) Borzęckiite, IMA 2018-46a, in: CNMNC Newsletter 70, Eur J Mineral 34
- WARR LN (2021) IMA-CNMNC approved mineral symbols. *Mineral Mag* 85: 291–320
- WOJDYR M (2010) Fityk: a general-purpose peak fitting program. *J Appl Crystallogr* 43: 1126–1128